Original Research Article

International journal of spray and combustion dynamics

International Journal of Spray and Combustion Dynamics
2016, Vol. 8(2) 86–99
© The Author(s) 2016
Reprints and permissions:
sagepub.co.uk/journalsPermissions.nav
DOI: 10.1177/1756827716640244
scd.sagepub.com

SAGE

Improving droplet sizing methodology for spray dynamics investigation

Jia Jie Woo, Vikram Garaniya and Rouzbeh Abbassi

Abstract

Spray modelling is one of the most useful techniques to characterize engine performance, efficiency and emissions. The size of droplets is one of the key variables that govern the efficiency of combustion of the liquid fuel. This study aims to develop an interactive tool using MATLAB codes that identifies the droplets and their sizes from the image taken with the long distance microscope in the spray chamber setup. In this developed method, firstly the background of the image was removed and then image processing techniques, *dilation* and *erosion,* were applied to the image file to refine the image files. Subsequently, *circle detection method* based on the *Hough Transform algorithm* with the function of *imfindcircles* was implemented. This function of the program allows the user to identify size droplets from the image files. A statistical study was conducted with the results automated from the MATLAB program using a different set of threshold values of black and white contrast. The results showed an optimal range for the threshold (black and white) values between 40 and 70. This optimal threshold range was established based on consideration of the correct and incorrect identification of the droplets. The results indicated that the program has the ability to identify the droplet providing size and numbers. The MATLAB program was developed using MATLAB compiler and can be used at different workstations.

Keywords

Spray dynamics, droplet sizing, image processing

Date received: 23 January 2015; accepted: 21 June 2015

Introduction

In global trade, the maritime transport industry plays an important role. The vessels used within the industry are usually powered by heavy duty, low to medium speed diesel engines. These types of marine diesel engine are one of the most efficient internal-combustion engines in the world, capable of delivering greater than 50% thermal efficiency.[1] Among the studies involving engine performance, efficiency and emissions, spray modelling of the liquid fuel is one of the main areas studied. The spray is influenced by a large number of parameters such as internal nozzle flow including cavitation, two-phase flow interactions, spray velocity profile, turbulence at nozzle exit, physical and thermodynamic states of liquid with surrounding gas, setting of equipment and the properties of droplets.[2,3] For example, the cavitation of the internal nozzle flow is considered to be the main reason for primary breakup which leads to atomization.[2–4]

In diesel spray injection, the fuel is injected into a high pressure chamber where the high pressure injection of fuel causes rapid disintegration of the liquid fuel into minute fine droplets ranging in size from 5 to 60 μm. There are numerous micro physical phenomena that occur from the nozzle to the disintegration of the liquid fuel into fine droplets. This disintegration process is also known as atomization of fuel.[1,5] The study of the diesel spray can be separated into two categories namely macro spray structure and micro spray structure. The studies of macro spray structure involve investigation of the spray structure as a whole. The method involves quantifying the shape and size of the spray and the effect of atmospheric pressure, viscosity and liquid surface tension on the spray size and shape.[1,5,6] The studies of micro spray structure and physics involve closer observations

Australian Maritime College, University of Tasmania, Launceston, Australia

Corresponding author:
Vikram Garaniya, Australian Maritime College, University of Tasmania, Launceston, TAS – 7250, Australia.
Email: v.garaniya@utas.edu.au

Creative Commons CC-BY-NC: This article is distributed under the terms of the Creative Commons Attribution-NonCommercial 3.0 License (http://www.creativecommons.org/licenses/by-nc/3.0/) which permits non-commercial use, reproduction and distribution of the work without further permission provided the original work is attributed as specified on the SAGE and Open Access pages (https://us.sagepub.com/en-us/nam/open-access-at-sage).

of the spray at microscopic scale. This is the main area of interest as it explains in more detail the causes of the macro spray structure formation. There are numerous fields of research found in literature, namely nozzle cavitation, breakup of liquid fuel, inter-droplet collision, the effects on drag coefficient from deformation of droplets, and the small-scale turbulent flow in the multiphase fluid mixture. These studies help understanding the micro physics of droplets interacting with gas and with other droplets.[1,5,6] As an example, Lin and Reitz[2] indicated that the viscosity tends to reduce the breakup rate and increase the drop size. Droplet sizing which is part of the turbulence modelling of liquid spray is one of the key variables that govern the combustion process.[5]

Nguyen et al.[7] noted that the study of fuel droplet evaporation and burnout in practical combustion systems via experimental and/or numerical means has been the focus of much research both past and present. This is because the engine power output and pollutant formation of the engine is strongly related to the fuel evaporation and burnout rates. It is essential to measure the fuel evaporation and burnout rates, and eventually these rates relate to the droplet sizing. Sirignano[8] stated that the droplet size is one of the key properties in measuring the rates of evaporation and burnout. As mentioned by Srinivasan,[9] large drops ignite late due to sustained local cooling from evaporation and small drops evaporate more quickly due to less significant local evaporative cooling. Sirignano[8] also concluded that the aerodynamic forces on a droplet depend on its size in a functional manner, which is different from the dependence of droplet mass on the size. As a result, smaller droplets undergo more rapid acceleration or deceleration than larger droplets. There are different correlations on the droplet sizing. Many different properties are used in the correlations such as viscosity, surface tension, orifice diameter, injection pressure, gas density and fuel density. Dam[6] concluded that many different setups and measuring positions are needed and a single correlation cannot be used.

There are three main measurement techniques used for sizing the droplets, phase Doppler interferometry (PDI), interferometric Mie imaging (IMI) and shadow imaging of particles.[10] These three techniques can be categorized into temporal or spatial sampling methods. Temporal sampling method can be explained as the measurement of drops in a fixed area during a specific time interval,[10,11] while spatial sampling method is instantaneous measurement of drops within a volume. It measures instantaneous size and velocity of spatially distributed droplets.[6] Berg et al.[10] theoretically described PDI as light scattering from spherical particles and showed that the phase shift of the light scattered from two intersecting beams can be used to accurately measure the diameter of spherical particles. PDI is also known as Phase Doppler Particle Analyser (PDPA).[11] Interferometric Mie Imaging (IMI) is also known as Interferometric Laser Imaging for Droplet Sizing (ILIDS) or Mie Scattering Imaging (MSI). As discussed by Fujisawa,[12] this sampling technique utilizes light scattering and interference for a 2D spray characterization. Berg et al.[10] also described the shadow imaging of particles which uses high-magnification optics to record the image with pulsed backlight illumination. This technique is an example of spatial measurement of volume defined by the focal plane and the depth of field of the imaging system.[10]

An experimental study was carried out by Bong[1] to validate the large eddy simulation full spray formation. This study explored dropsize shadowgraphy technique using high pressure spray chamber (HPSC) with a dual-frame CCD camera, a double-pulse 120 mJ laser with light sheet optics, a high-efficiency diffuser and an acquisition computer.[1] With the aid of a long distance microscope dropsize images of spray at a specific location were obtained and then these images were analysed with a combination of software namely; DaVis v7.2 and MATLAB v7.5. Bong[1] stated that there were issues with this droplet sizing technique, which produced differences between the mean values of the measured droplets. Bong[1] presumed that the errors were caused by limited sample size, low quality images taken in the dense part of the spray and limited precision from the camera and lens for measurement of small droplets.

Advancing from the physics of a diesel spray and the droplet sizing techniques, Bong's experimental study showed the validation of the large eddy simulation full spray formation. However, the results were affected by the limitation of the software DaVis v7.2.[1] The software was unable to produce an accurate result and was unable to identify all the droplets from the image files. The algorithm used within the software was only able to identify the droplets with a significant contrast between the droplet and background. Some images taken from the HPSC are from the dense part of the spray where contrast between backgrounds does not exist. Therefore, the aim of this study is to develop an interactive program using MATLAB to improve the algorithm of the program. This is undertaken to make an improvement in analysing the images.

Methodology

This section provides the steps followed to identify the droplets within the image file. The logical flow chart of the methodology is shown in Figure 1. The first step is to remove the background from the image file. This process significantly improves the contrast between the droplet and the background. Subsequently, the

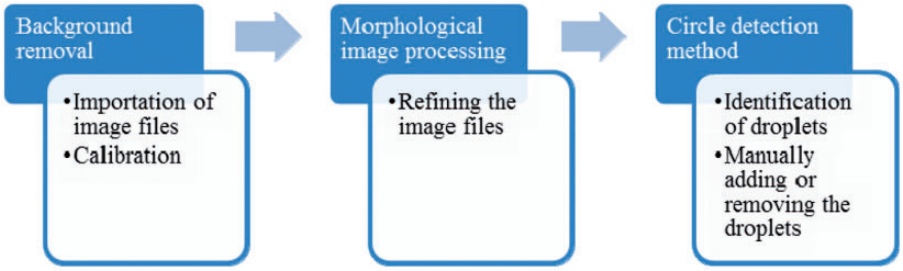

Figure 1. Logical flow chart of the methodology.

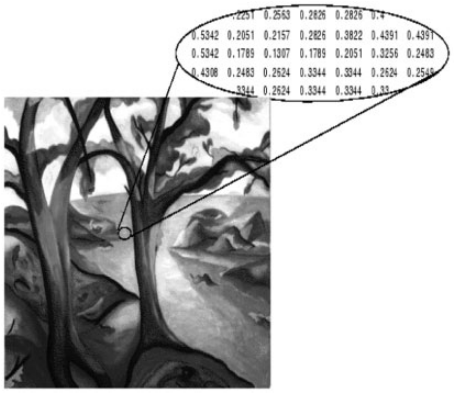

Figure 2. Example of a grayscale type image.[14]

image processing techniques *opening*, *closing* and *reconstruction* are applied. This improves the results by refining the image file so that a clearer representation of the droplet can be produced. Once the image is refined, the next phase of the program is to identify the droplet from the image files. Two approaches were taken during the research which included the *edge finding method* and *circle detection method*. All the approaches and steps are outlined in the following subsections.

Background removal

For the digital image process, there are four basic types of images defined within MATLAB software these being binary, indexed, grayscale and true colour.[13] These image types determine the way MATLAB interprets the data matrix elements as pixel intensity values. The program created in this project requires the image files in grayscale type. Values from 0 to 1 or 0 to 255 can be used to define the intensity value of pixel in the image[13] where value 0 represents black and value 1 or 255 represents white. There are three types of class array used to refine the matrix of image file such as double, uint8 or uint16.[14] A class array of double shown in Figure 2 gives a range of 0 to 1, while uint8 and uint16 give a range of 0 to 255 for the intensity values.

In order to remove the background from the image file, a threshold value between 0 and 255 needs to be applied to define the maximum intensity value of the droplet. This value is chosen based on visual inspection by the user. The pixels with intensity value higher than the threshold value are converted to 255 which are represented as white and the pixels lower than the threshold value are converted to 0 which are represented as black.

Morphological image processing

In the next step, image processing techniques *opening*, *closing* and *reconstruction* are applied to the image with better contrast from the background removal process. These image processing techniques are based on the fundamental of image processing morphology, *dilation* and *erosion*. *Dilation* is an operation that 'grows' or 'thickens' objects in the image.[15,16] As shown in Figure 3, *dilation* of A by B is the set consisting of all the structuring element origin locations where the reflected and translated B overlaps some portion of A. E*rosion* 'shrinks' or 'thins' the object in the image.[15,16] Figure 4 is showing *Erosion* of A by B. It is the set of all structuring element origin locations where the translated B has no overlap with the background of A. The operations of *dilation* and *erosion* are used in combinations for the *opening* and *closing* applications. The *morphological opening* of A by B is defined as the *erosion* of A by B then followed by the *dilation* of the results by B. The *morphological closing* of A by B is a *dilation* of A by B followed by *erosion*.

The example of *opening* and *closing* is shown in Figure 5 where subfigure (b) shows the results of *opening* in which the thin protrusions and outward pointing boundary irregularities are removed. The thin join and the small isolated object are also removed. Subfigure (c) is showing the result of closing where the thin gulf, the inward-pointing boundary irregularities, and the small hole, are removed. Finally, subfigure (d) shows that the combination of *opening* and *closing* gives a smoothed object compared to the original image.

Morphological reconstruction is another image processing technique that can be applied in the program

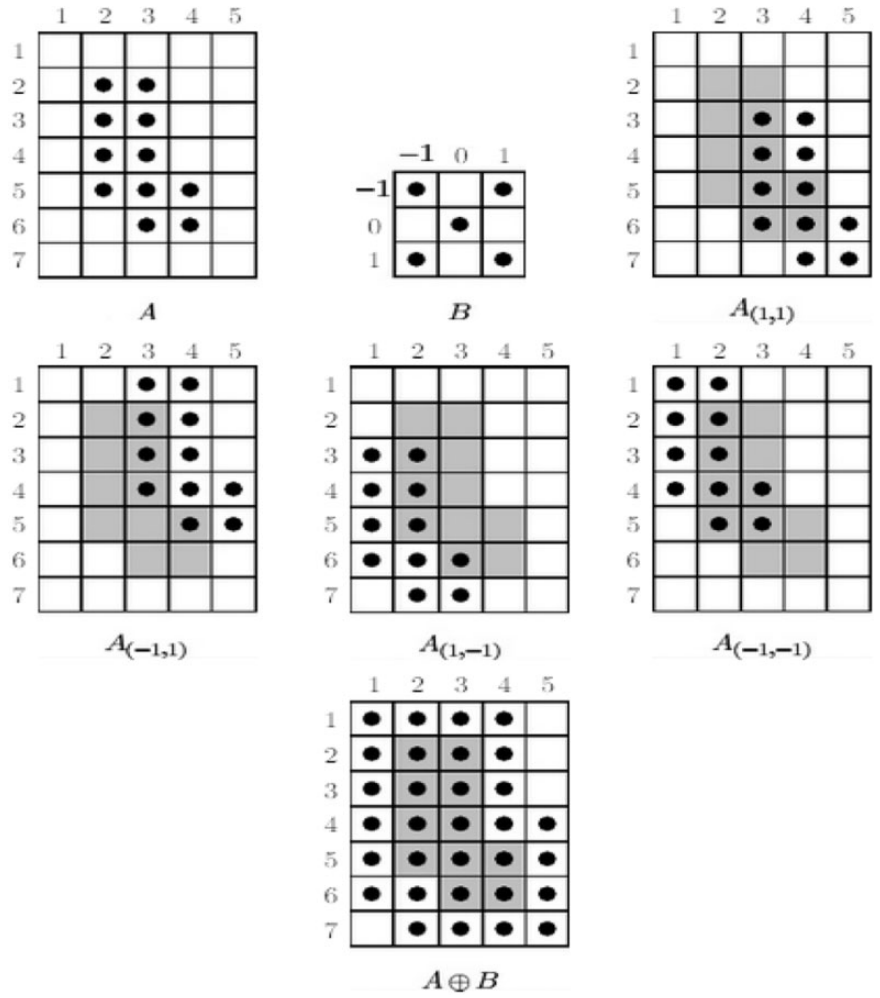

Figure 3. Example of dilation.[16]

where it involves two images and a structuring element.[15,16] This is the difference between *reconstruction* and the combination of *opening* and *closing*, as *opening* and *closing* used a single image and structuring element. In *reconstruction*, one image is used as the marker that undergoes the transformation of *opening* and *closing* while the other image is used as the mask which constrains the transformation.[15] Figures 6 and 7 shows an example of the morphological reconstruction where the border characters are removed.

Edge finding method

Once the image is refined, the initial approach is to identify the edge of the droplet to determine its size. There are several methods that can be applied to determine the edge of the droplet such as *Sobel*, *Prewitt*, *Roberts*, *Laplacian of Gaussian*, *Zero-cross* and *Canny*. *Sobel* method is the default method used in MATLAB where it performs a 2D spatial gradient measurement on the image and emphasizes regions of high spatial frequency that correspond to edges.[17] It is used to find the approximate absolute gradient magnitude at each point in the input grayscale. However, with the edges of the droplet identified, it is challenging to obtain information that is useful to determine the size of the droplet. The edges identified are in a non-uniform shape and further research needs to be undetaken in order to refine the non-uniform edge into a uniform circular shape. During the research, a better approach was discovered. This is discussed next.

Circle detection method

Yuen et al.[18] described a number of circle detection methods available based on the variations of *Hough Transforms* such as *standard Hough Transform*, *Fast Hough Transform*, *Gerig and Klein Hough Transform*, and a *two stage method*. A function of *imfindcircles* based on a *Circle Hough Transform* (CHT) algorithm

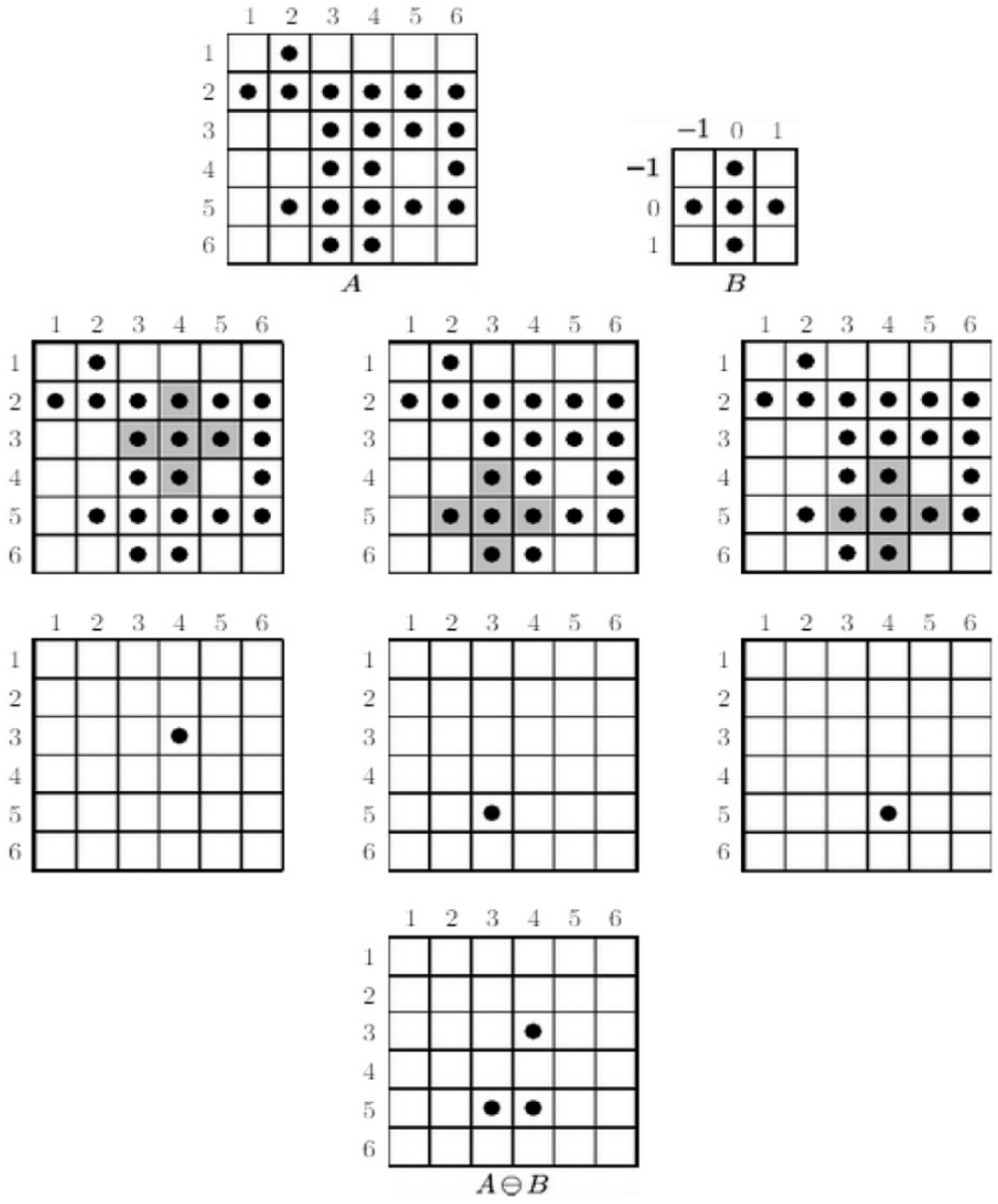

Figure 4. Example of erosion.[16]

to identify the circles in images was implemented.[19] Although the CHT is not a rigorously specified algorithm compared to those mentioned previously, there are essential steps which are common to all the different approaches that can be taken, such as accumulator array computation, centre estimation and radius estimation.

The accumulator array computation begins with the estimation of gradient for the pixels within the image. Then the gradient value calculated is used to identify the edge pixels in the image. The foreground pixels of high gradient are designated as being the candidate pixels to cast 'votes' in the accumulator array. These candidate pixels voted in pattern around them forms a full circle of a fixed radius.[19] Figure 8(a) shows an example of a candidate pixel lying on an actual circle (solid circle) and the CHT voting pattern (dashed circles) for the candidate pixel. The votes of candidate pixels belonging to an image circle tend to accumulate at the accumulator array bin corresponding to the circle's centre. Therefore, the circle centres are estimated by detecting the peaks in the accumulator array. Figure 8(b) shows how an example of the candidate pixels (solid dots) lies on an actual circle (solid circle)

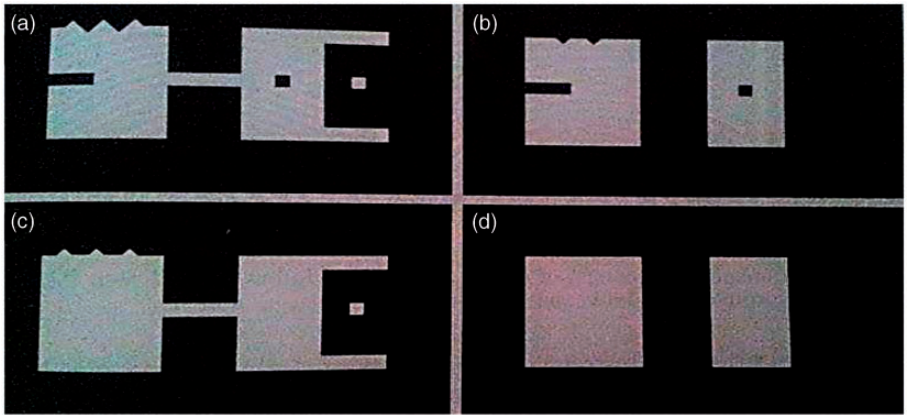

Figure 5. Example of opening and closing. (a) Original image, (b) Opening, (c) Closing, (d) Closing of (b).[16]

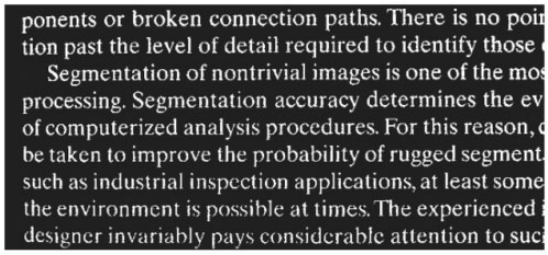

Figure 6. Original image before morphological reconstruction.

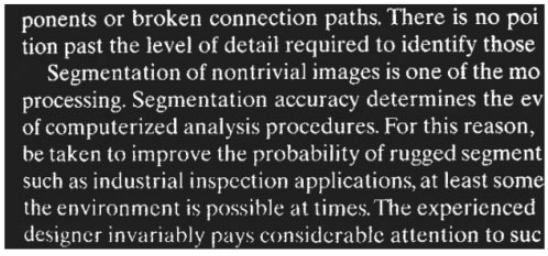

Figure 7. The image after morphological reconstruction with border characters removed.

and their voting patterns (dashed circles) which coincide at the centre of the actual circle. Afterward, the radius is estimated by decoding the phase information from the estimated centre location in the accumulator array.[19,20]

Results

This section is divided into four parts, in the first part a step-by-step process of droplet sizing using the MATLAB program is described. The second and third part give a statistical study and the confidence interval is described and the fourth part is discussion regarding the outcome of the program.

Step-by-step process

The program was created using a graphical user interface (GUI) design environmental function with MATLAB version 2013b. In the GUI, a graphic is displayed in one or more windows containing controls called components that enable a user to perform interactive tasks.[21] The main advantage of using a GUI is that it does not require the user to create a script or type commands at the command line to accomplish the tasks. This allows the user to run the program without programming knowledge.

Figure 9 shows the interface of the program where the controls such as the file browsing button, calibration button, etc. are located on the right hand side. The results are shown on the left hand side with the plots, together with text and table providing the information on the size and number of droplets. After loading the images, the calibration image needs to be imported. The calibration function allows the user to manually select two points to define a certain length of the line as shown in Figure 10(a). This calibration information is then stored and used to calibrate the other images selected, as shown in Figure 10(b).

The program then filters out the background using a threshold value between 0 and 255. The threshold value can be adjusted by changing the slider within the red region area in the program interface. Figure 11 shows the result after applying the threshold value. It can be clearly observed that the background is removed, and a significant contrast between the droplet and background is displayed. Figure 12 shows the refined image, clarified by image enhancement. It can be seen that it filled the gaps within the droplets and helped to emphasize the boundary. The program is then able to identify the droplets with the *imfindcircles* function. Figure 13 shows the results of the function where four droplets are recognized and the size of each is presented in the table beneath the refined image.

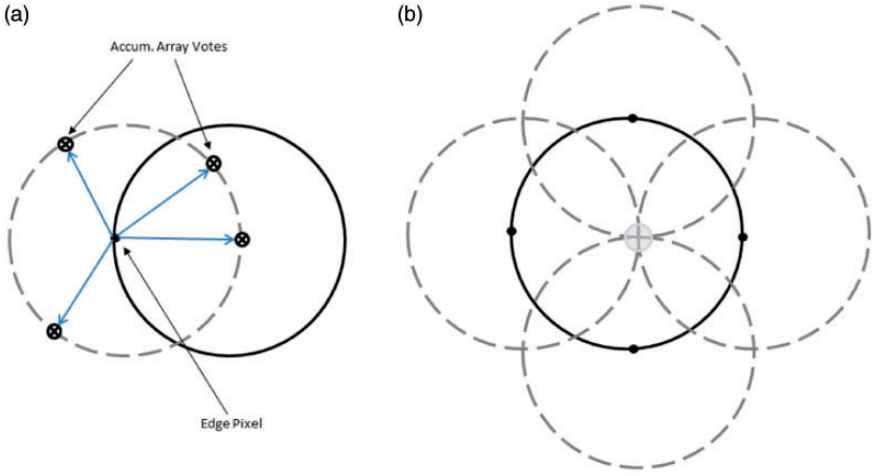

Figure 8. CHT voting pattern.[20]

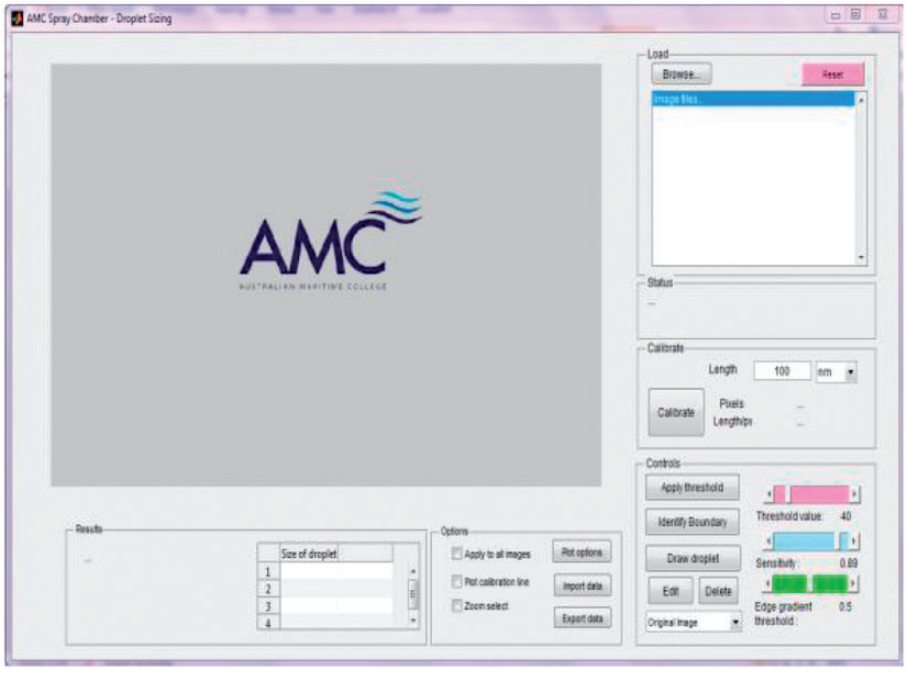

Figure 9. Interface of the program.

Moreover, in order to ensure that the results obtained are accurate and realistic, the program allows the user to manually add, edit or delete the identified droplets. Figure 14 shows the process of manually adding a measured droplet, indicated by the arrow within the figure. This function allows the user to select the centre and the edge of the droplet and then draw an adjustable circle. Figure 15 show the editing and deleting function.

The program includes import and export functions for storing or modifying the results. This allows the measured droplets in the image to be imported or exported and thus be compared with the results obtained different settings. Figure 16 shows the import function that allows the user to select the measurement data file from a folder to be imported.

The Export function saves the measurement data file into a user selected folder. Furthermore, image files

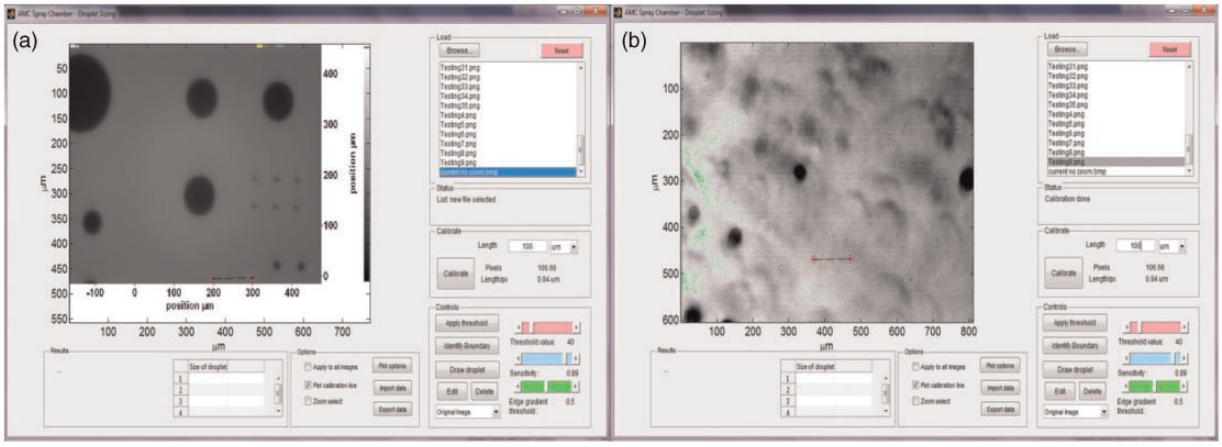

Figure 10. (a) Calibration process. (b) Calibrated image file.

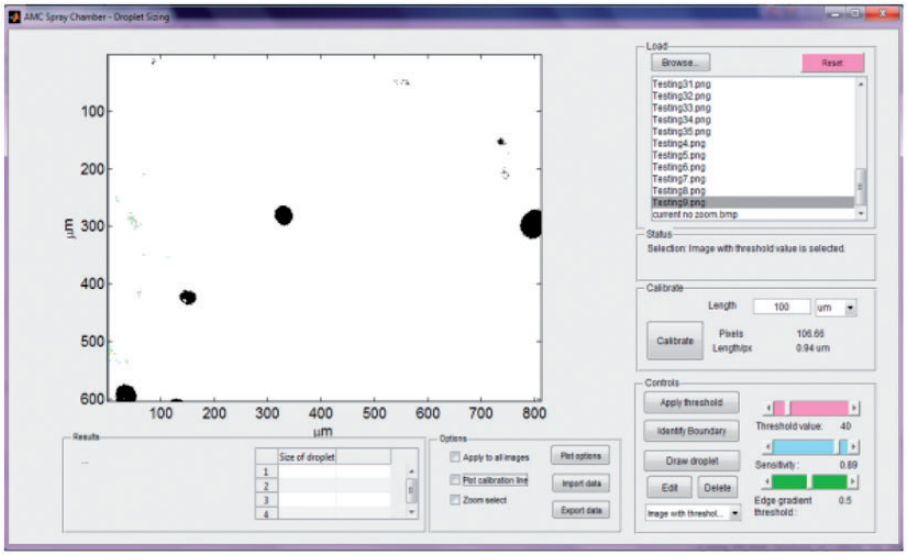

Figure 11. Threshold value applied and showing the image with background removed.

with different settings are used to validate the algorithm of the program. As shown in Figure 17, two image files with different threshold values are imported as an example, and then analysed.

Statistical study

As shown in Figure 17, different threshold values identify different numbers of droplets. Therefore, a statistical study is carried out to examine the results over a range of threshold values. The sensitivity factor value and edge gradient threshold value are kept constant at 0.87 and 0.5 during the results evaluation process. The sensitivity factor is the sensitivity for the circular Hough transform accumulator array. The higher sensitivity value implies that more droplets can be identified. However, with the higher sensitivity, there is an implicit risk of detecting false droplets. The edge gradient sets the threshold for determining edge pixels in the image. The lower edge gradient threshold can help to detect more droplets with a weaker edge and vice versa.

In order to evaluate the results and make a comparison, a set of measurement data was manually identified by human eye. This set of measurement data is then used as the sample data to compare with the results using different threshold values. The testing range of the threshold value was between 20 and 120, and the standard deviation and mean was calculated for each set of these values, using equations (1) and (2).

$$\text{Mean}, (\bar{x}) = \frac{1}{N}\sum_{i=1}^{N} x_i \tag{1}$$

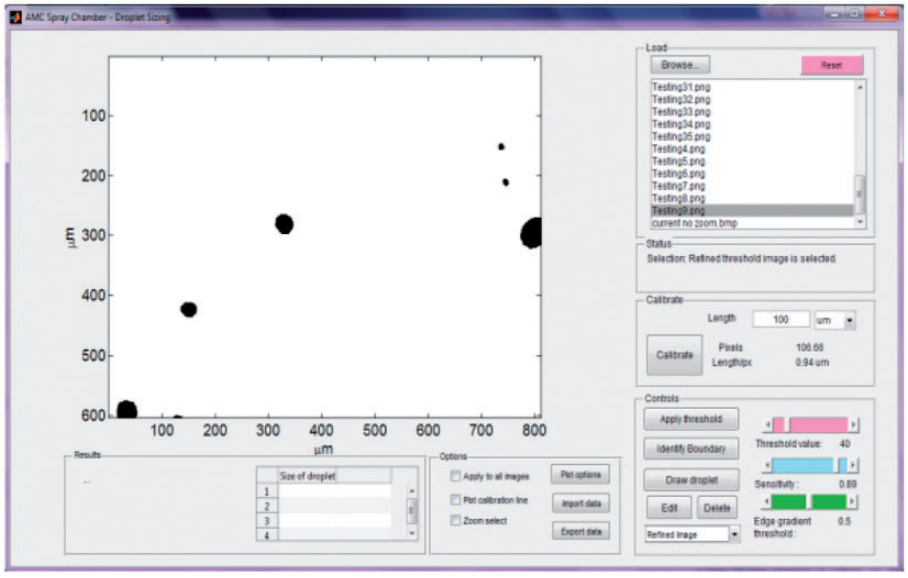

Figure 12. Displaying the refined image.

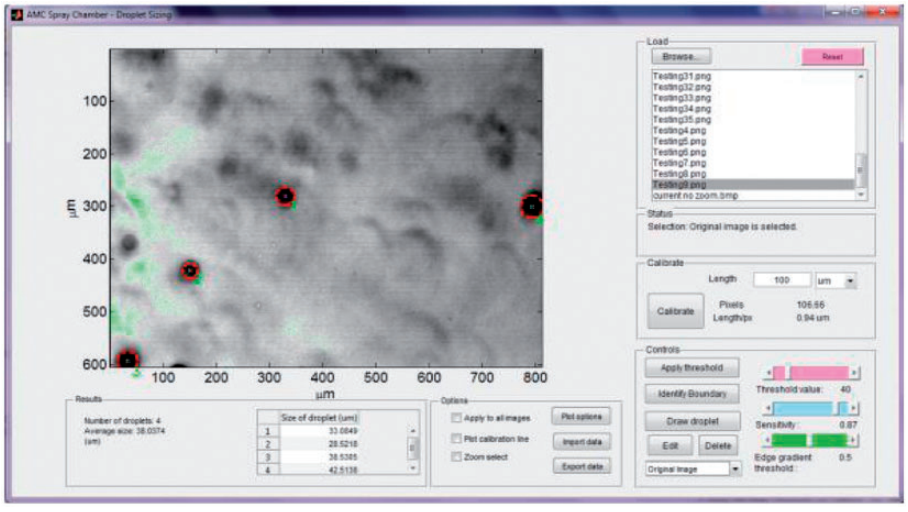

Figure 13. Identification of droplets with the original image as background.

$$\text{Standard deviation}, (\sigma) = \sqrt{\frac{1}{N}\sum_{i=1}^{N}(x_i - \mu)^2} \quad (2)$$

The normalized standard deviation and mean in terms of percentage with the mean of sample data is given as equations (3) and (4)

$$\text{Normalised standard deviation}, (\sigma_N) = \frac{\sigma}{\bar{x}_{manual}} \times 100\% \quad (3)$$

$$\text{Normalised mean}, (\bar{x}_N) = \frac{\bar{x}}{\bar{x}_{manual}} \times 100\% \quad (4)$$

Figure 18 shows the normalized mean and standard deviation over the range of threshold values for the correct and incorrectly identified droplets.

For the right or correct identification of the droplets, the highest normalized mean is around 52% when the threshold value is between 70 and 80. The normalized standard deviation for correct identification is in between 15% and 31%. While for the incorrect identification of the droplets, the normalized mean increases along with the threshold value. The normalized standard deviation is in between 7% and 38%.

Confidence interval

According to the central limit theorem, the sampling distribution of a statistic follows a normal distribution.

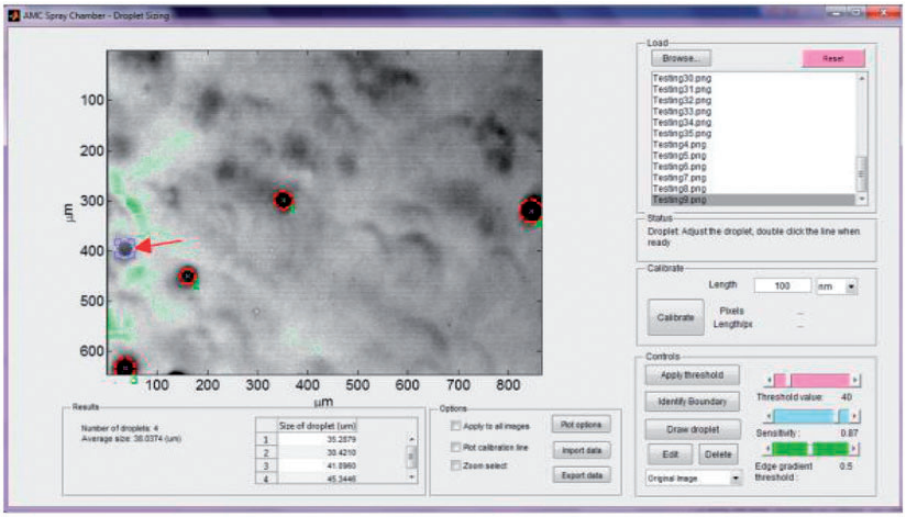

Figure 14. Manual edit of unidentified droplets.

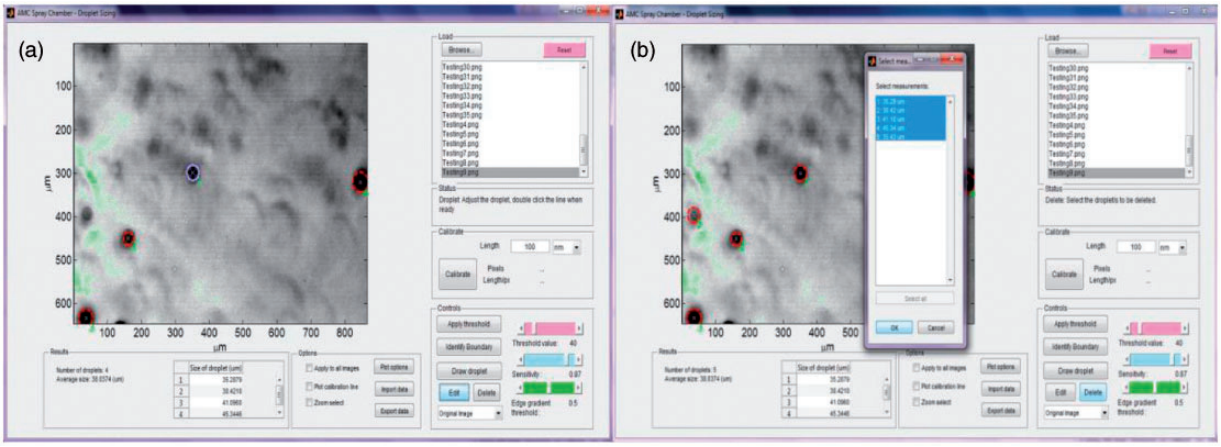

Figure 15. (a) Editing the droplets. (b) Deleting the droplets.

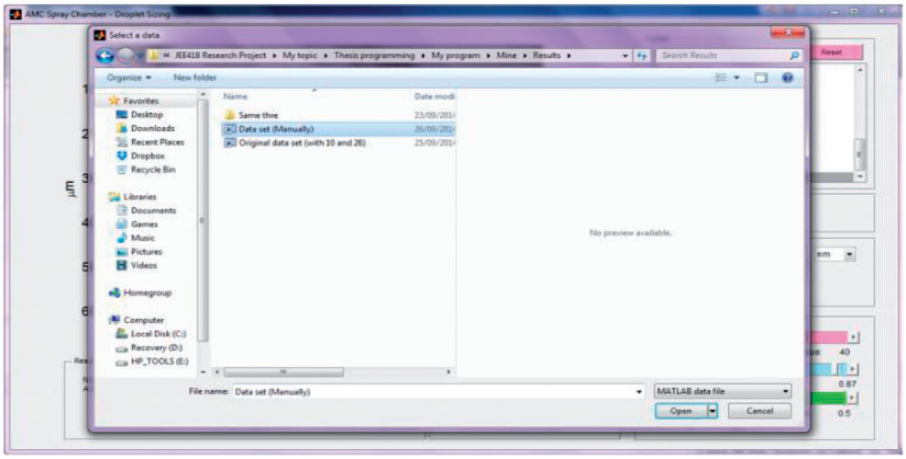

Figure 16. Data importing.

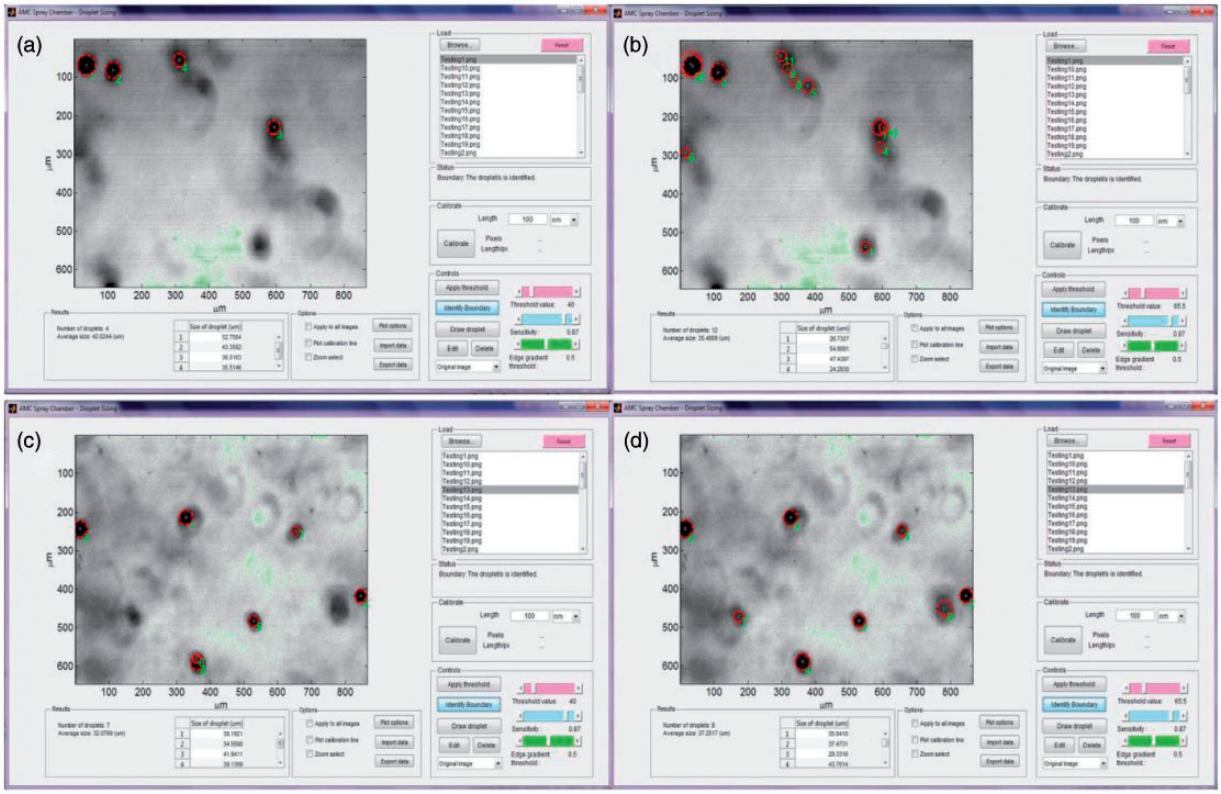

Figure 17. Examples of image files with different threshold values (40 and 65.5).

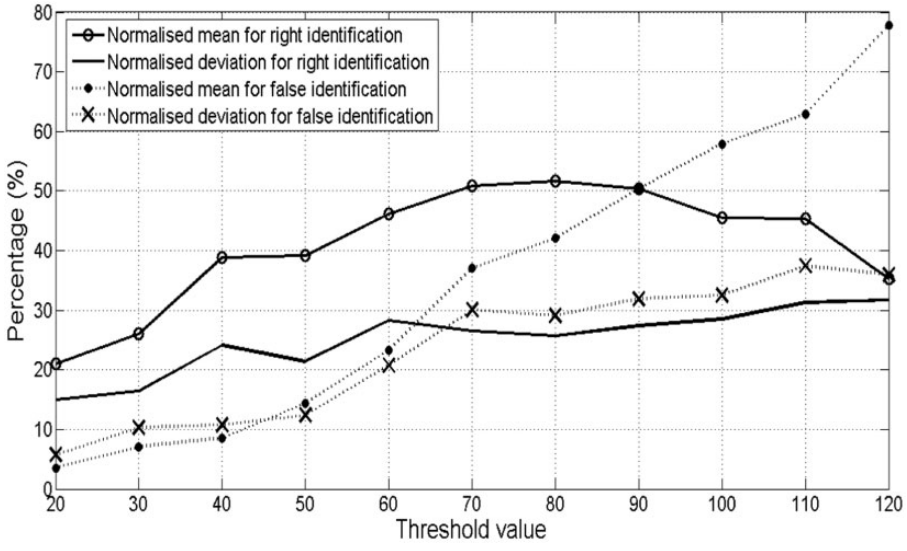

Figure 18. The normalized mean and deviation for the right and false measurement.

A *t*-distribution which is known as the Student's *t*-distribution is used to determine the confidence interval for the mean value of each threshold value set. It is a probability distribution that is used to estimate population parameters when the sample size is small.[22] The *t*-scores are the standardized scores on each element for a set of samples. This standardized score can be used to evaluate the probabilities with the sample mean by knowing the standard deviation. The formula for *t*-scores is expressed as

$$t\text{-score},\ (t) = \frac{\bar{x} - \mu}{s/\sqrt{N}} \tag{5}$$

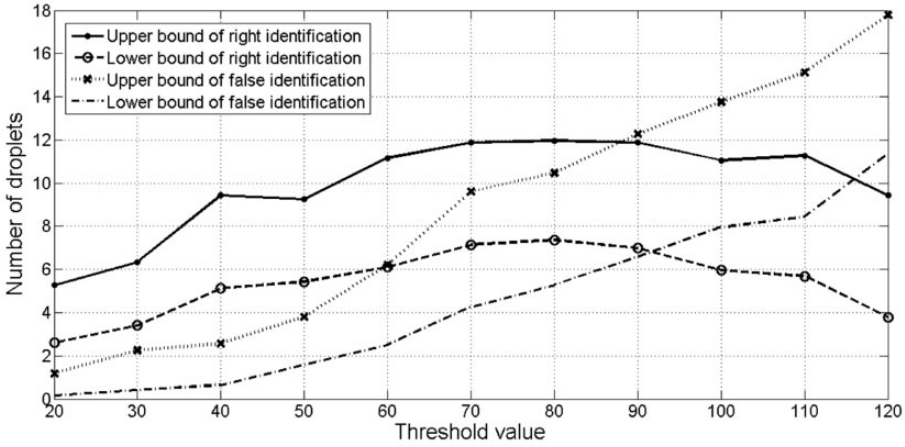

Figure 19. The 99% confidence interval for the droplets identified for each set of threshold values.

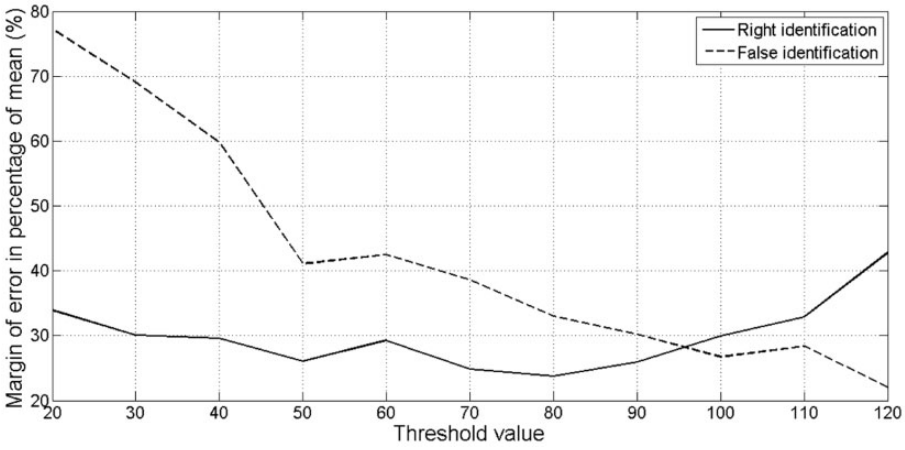

Figure 20. Margin of error in percentage of calculated mean for each set of threshold values.

A confidence interval can be formed with the *t*-score to describe the amount of uncertainty associated within the sample. For example, a 99% confidence interval on the estimation of the mean indicates that 99% of the intervals would include the mean denoted as $\bar{x} \pm E_{.99}$ The term $E_{.99}$ is known as the margin of error which is also $(\bar{x} - \mu)$ in t-score formula that calculated as

$$\text{Margin of error}, (E_{.99}) = \textit{critical value} \times \frac{s}{\sqrt{N}} \quad (6)$$

where the critical value is the *t*-score from *t*-distribution calculated using a confidence level of 99% and degrees of freedom with 32, *s* is the standard deviation and *N* is the sample size. It is assumed that the results to follow a normal distribution curve. The margin of error is then expressed as a percentage of the mean which is calculated as

$$e_{.99} = \frac{E_{.99}}{\bar{x}} \times 100\% \quad (7)$$

Figure 19 shows the confidence interval for the mean value of droplets identified for each set of threshold values. This gives an estimation of range for the mean value of correct or right identified droplets. The highest numerical value of the interval is between 7 and 12 droplets when the threshold value is 80. The figure also indicates that the value of estimation for mean value of incorrect (false) identified droplet rises with higher threshold value.

Figure 20 shows the margin of error in the percentage of calculated mean with the threshold value between 50 and 90 shows a lower percentage of error for correct and incorrect identification compared to other regions. The decline of the percentage for the false identification is due to the higher value of false identification when threshold value increases.

Discussion

Based on the results, it is found that the threshold value of 10 would be too low to be applied as the program

will identify a droplet with a dimension even smaller than 5 μm. Furthermore, it is also noted that the threshold value of 130 would be too high to be applied. This is due to the high degree of inaccuracy where most of the identified droplets are anticipated to be false droplets. Hence, a threshold value between 20 and 120 is used in the statistics study.

The optimum range of the threshold value can be narrowed down based on the results from the statistical study. As shown in Figure 18, the program had higher chances of identifying the correct droplets until it reached a maximum point. The program tends to identify more false droplets as the threshold value increases. A threshold value of 40–70 is considered to be the optimum range here as it gives a higher value of the normalized mean and lower value of the normalized standard deviation for the right identification. Likewise, it gives a slightly lower value of the normalized mean and standard deviation for the false identification. This indicates the program is performing better with less variation of error and higher number of right identifications.

As shown in Figure 19, a threshold value between 40 and 70 provides a higher percentage for recognizing the correct fuel droplets. Looking at the margin of error in the confidence interval in Figure 20, indicates that the threshold value of 50–90 gives the lower percentage in term of the mean for the right identification. This shows that the program is more reliable in that range as it is able to produce fairly consistent results with smaller margin of error over the samples. Based on the results from the statistical study, it can be concluded that the optimum range of the threshold value is around 40–70.

Figure 18 shows that the highest normalized mean for the right identification is around 52% which is around half of the sample mean value. In reality, the result varies depending on the judgment of the human eye when creating the manual data set, as errors can be made by missing some droplets or considering too many of the unclear or unsure droplets as real droplets. This relates to the limitation of previous software DaVis v7.2 where the program was unable to identify most of the droplets with an image file taken from the dense part of the spray. A justification can be made regarding this issue which is related to the 'intensity profile' of the pixels within the image. The program often does not identify some of the droplets supposed to be correct based on the human eye. This is due to the method of the interpolation process for the droplets. The human eye is unable to recognize the intensity level limiting differentiation of black and white only while the program is able to differentiate based on the pixel intensity.

The problem then arises that the image files imported into the program should have a clear contrast between the droplet and the background. The developed MATLAB program gives a better approach compared to the DaVis software regarding this issue. The program allows more flexibility in terms of obtaining the results with a huge number of combinations with different values of threshold, sensitivity factor and edge gradient threshold. The program can be utilized to detect and determine the number and size of the droplets over the image files with different characteristics as well.

The program is developed into two version of self-extracting archive where one is for the user with MATLAB software installed in the workspace and the other is for the user without MATLAB software. The user with MATLAB installed can install the MATLAB program that develops and also creates a shortcut icon on their desktop. The user without MATLAB installed will require installing the MATLAB Compiler Runtime. This allows the MATLAB program to run, even without the MATLAB in the workstation. The installed MATLAB program folder will contain a number of files including the user manual pdf file. The user manual file explains the process from setting up the program, launching the program, how to begin the program and a step by step guide for troubleshooting.

The program is tested with different workstations that use various operating systems and hardware to ensure the compatibility and usability of the developed program. It is supported by several operating systems such as Microsoft Windows 2003 to Windows 8, Mac OS X 10.7.4+ to 10.9, Linux Debian 6.x to Qualified distributions as long the MATLAB Compiler Runtime or Mathworks MATLAB software 2013b above is pre-installed.

Conclusions

The developed program showed good correlation of results, and demonstrated its ability to identify droplet size and distribution in the fuel aerosol. Moreover, the program also provides the ability to add, edit or delete the identified droplets. The flexibility of the program is another main feature which allows the user to define different setting that may be applied to different images such as an image file taken from a highly dense part of the spray. In conclusion, the program has proven its compatibility and usability from the testing and its accuracy from the statistical study. However, some modifications are needed to the program, in order to obtain more accurate results from the image files. The suggestion for further work would be to add another function to merge the results in the program. This would allow improved outcomes by combining the results from different settings, such as a higher sensitivity value or a lower edge gradient threshold. This practice would result in optimizing the outcome performance of program for image files with different features.

Declaration of conflicting interests

The author(s) declared no potential conflicts of interest with respect to the research, authorship, and/or publication of this article.

Funding

The author(s) received no financial support for the research, authorship, and/or publication of this article.

References

1. Bong CH. Numerical and experimental analysis of diesel spray dynamics including the effects of fuel viscosity. PhD thesis. University of Tasmania, Australia, 2010.
2. Lin SP and Reitz RD. Drop and spray formation from a liquid jet. *Annu Rev Fluid Mech* 1998; 30: 85–105.
3. Badock C, Wirth R, Fath A, et al. Investigation of cavitation in real size diesel injection nozzles. *Int J Heat Fluid Fl* 1999; 20: 538–544.
4. Dabiri S, Sirignano WA and Joseph DD. Cavitation in an orifice flow. *Phys Fluid* 2007; 19: Paper no 072112.
5. Weisser A. *Modelling of combustion and nitric oxide formation for medium-speed DI diesel engines: a comparative evaluation of zero- and three-dimensional approaches*. Zurich: Swiss Federal Institute of Technology, 2001, p.252.
6. Dam BS. Experimental and numerical investigations of sprays in two stroke diesel engines. PhD thesis. Department of Mechanical Engineering, Technical University of Denmark, Denmark, 2007, p. 186.
7. Nguyen D, Honnery D and Soria J. Magnified digital inline holographic measurement of micro droplets. In: *Fifth Australian conference on laser diagnostics in fluid mechanics and combustion*. Perth, Australia: The University of Western Australia, 2008, p.4.
8. Sirignano WA. *Fluid dynamics and transport of droplets and sprays*. Cambridge, UK: The University of Cambridge, 1999, p.309.
9. Srinivasan S, Rutland CJ and Wang Y. *Fundamental simulations of mixing and combustion of turbulent liquid sprays*. Engine Research Center, University of Wisconsin–Madison, 2007, p.28.
10. Berg T, Deppe J, Michaelis D, et al. Comparison of particle size and velocity investigations in sprays carried out by means of different measurement techniques. In: *International conference on liquid atomization and spray systems*. Goettingen: LaVision GmbH, 2006, p.7.
11. Palacios E, Lecuona A and Rodríguez PA. *On the experimental determination of the measurement volume diameter in the PDA technique*, Lisbon, Portugal, 2004, p.6.
12. Fujisawa N, Hosokawa A and Tomimatsu S. Simultaneous measurement of droplet size and velocity field by an interferometric imaging technique in spray combustion. *Meas Sci Technol* 2003; 14: 10.
13. MathWorks. Image types in the toolbox, http://www.mathworks.com.au/help/images/image-types-in-the-toolbox.html (2014, accessed 1 June 2014).
14. MathWorks. 8-Bit and 16-bit images, http://www.mathworks.com.au/help/matlab/creating_plots/working-with-8-bit-and-16-bit-images.html (2014, accessed 1 June 2014).
15. Gonzalez RC, Woods RE and Eddins SL. *Digital image processing using MATLAB*. Upper Saddle River, NJ: Pearson Prentice Hall, 2004.
16. McAndrew A. An introduction to digital image processing with Matlab notes for scm2511 image processing 1, http://www.scribd.com/doc/99090940/53/Edge-enhancement (accessed 25 May 2014).
17. Fisher R, Perkins S, Walker A, et al. Sobel edge detector, http://homepages.inf.ed.ac.uk/rbf/HIPR2/sobel.htm (2003, accessed 15 June 2014).
18. Yuen H, Princen J, Illingworth J, et al. Comparative study of Hough transform methods for circle finding. *Image Vision Comput* 1990; 8: 71–77.
19. MathWorks. Find circles using circular Hough transform, http://www.mathworks.com.au/help/images/ref/imfindcircles.html (2014, accessed 20 June 2014).
20. Davies ER. *Machine vision: theory, algorithms, practicalities*. St. Louis: Elsevier, 2004.
21. MathWorks. What is a GUI? http://www.mathworks.com.au/help/matlab/creating_guis/what-is-a-gui.html (2014, accessed 30 May 2014).
22. StatTrek.com. Student's *t*-distribution. Teach yourself statistics, http://stattrek.com/estimation/confidence-interval.aspx (2014, accessed 30 August 2014).